Indian J Phys (September 2020) 94(9):1451–1456
https://doi.org/10.1007/s12648-019-01567-8

ORIGINAL PAPER

Investigation of accelerated carbon ions with the presence of QED effect by ultra-intense high-power lasers

O Culfa[1,2]* and V Sert[2]

[1]Department of Physics, University of Nebraska-Lincoln, Lincoln, NE, USA

[2]Department of Physics, Karamanoglu Mehmetbey University, Karaman, Turkey

Received: 23 March 2019 / Accepted: 06 June 2019 / Published online: 20 July 2019

Abstract: In this study, we have investigated carbon ions, fast electrons and gamma-ray energy spectra and the corresponding temperatures when next-generation 10 petawatt (PW) lasers (irradiances of 5×10^{22} W cm^{-2}) hit solid targets with a preformed plasma at the front surface. We employed 2D particle-in-cell (PIC) code with the presence of quantum electrodynamics (QED) effects. The maximum energy reached by the accelerated particles, and the corresponding temperature due to nonlinear plasma processes can be affected by varied plasma scale lengths. Here, we show the effects of varied plasma scale lengths on particle acceleration at irradiances on the order of 10^{22} W cm^{-2}, which is a new development for laser technology. We have observed that fully ionized carbon ions can reach up to 2.5 GeV energies with an optimum plasma scale length of 1 μm and the corresponding temperature of 40 MeV. Accelerated electron energies reach up to 1.5 GeV with the temperatures of 50 MeV for 10 PW laser–plasma interactions with the presence of QED effects. We have demonstrated that by varying plasma scale length, heavy ion energy and temperature can be controlled, which is important for various applications such as hadron therapy and X-ray imaging.

Keywords: Laser–plasma interactions; Particle acceleration; PIC simulations

PACS Nos.: 41.75.Jv; 52.38.-r; 52.38.Ph; 52.50.Jm

1. Introduction

Developing technology of high-power lasers will allow us to reach the power of 10 PW laser systems in the foreseeable future and such high-power laser systems are currently under construction in ELI projects [1]. 10 PW ultra-intense high-power lasers will give us the opportunity to investigate particle acceleration with the presence of quantum electrodynamic (QED) effects. Ultra-intense high-power laser pulses have strong electromagnetic fields which rapidly ionize matter to produce a plasma. The generated electromagnetic fields in this plasma can accelerate charged particles (electrons and ions) to high energies over very short distances [2, 3]. High-power laser–plasma interactions therefore have potential application ranging from hadron therapy [4] and X-ray imaging [5] to next-generation particle accelerators [6–8]. With the development of multi-petawatt-class lasers, intensities of $\sim 10^{23}$ W cm^{-2} will be reachable, giving rise to a new regime in which interesting new physics becomes accessible. This includes the acceleration of ions to GeV energies by the light pressure of the laser [9] and the onset of nonlinear QED effects which produce emitted photons created by electron–positron pairs on interaction with the laser fields (multi-photon Briet–Wheeler pair production) [10–12]. The dynamics of plasmas generated by next-generation 10 PW lasers will be dominated by these emission processes [13–15]. Recent computational studies have shown that quantum radiation reaction and multi-photon Briet–Wheeler pair production have a strong influence on particle acceleration in multi-petawatt laser–solid interactions [16, 17]. In this study, the generation of carbon ions, hot electrons and photons in ultra-intense ($> 10^{22}$ W cm^{-2}) laser–plasma interactions for different preformed plasma scale lengths and at the presence of QED effects has been investigated.

We have used 2D EPOCH particle-in-cell (PIC) code to simulate 10 PW laser–solid interactions with an

*Corresponding author, E-mail: ozgurculfa@unl.edu

exponential preformed density profile [18, 19]. Here, we have investigated the effect of varied plasma scale length (L) from 0 to 10 μm on particle acceleration in multi-petawatt laser–plasma interactions ($I \sim 10^{22}$ Wcm $^{-2}$) when the QED effect is present.

2. EPOCH 2D PIC code simulations

We performed 2D EPOCH PIC simulations of laser–solid interactions with a preformed plasma in front of the target. The system size was varying from 13 μm × 74 μm with a mesh resolution of 20 nm cell size and 100 particles in each cell, comprising of electrons and carbon ions.

The simulated laser irradiance was 5×10^{22} W cm^{-2} with a linear polarized beam focused to a 3 μm focal spot with an incidence angle of 0°. The laser wavelength and pulse duration were 0.82 μm and 25 fs, respectively. The peak electron density was limited to 7×10^{29} m^{-3}. The target was assumed to be fully ionized carbons with a thickness of 0.5 μm. For pre-plasma, the density profile can be defined as $n_e = n_s \exp(-x/L)$ where, n_e is the electron number density, n_s is solid density, and L is the plasma scale length. The plasma scale length (L) was varied from $L = 0$ to $L = 10$ μm with a cutoff to zero density at 0.1 n_c, where n_c is the critical density.

For irradiances greater than $\sim 10^{22}$ W cm^{-2}, we expect radiation pressure ion acceleration (RPA) [16, 20, 21] to dominate the acceleration of protons and heavy ions. Figure 1 shows the average kinetic energy of the simulated carbon ions at different time steps for 1 and 5 μm preformed plasma scale lengths in front of the target. Initially, the carbon ions are accelerated at the front surface of target, indicating that RPA is the accelerating mechanism. Later, accelerated electrons at the front surface set up a shield field behind the target and lead the second acceleration mechanism at the rear surface which is called target normal sheath acceleration (TNSA) mechanism. The ions are accelerated at the front surface of the target, indicating that RPA is the accelerating mechanism initially, then TNSA effect was present which shows that ions are accelerated at the back of the target which is called hybrid mechanism [22].Therefore, electrons accelerated by the laser set up a sheath field and other particles are accelerated by this sheath field in the target normal direction to higher energies as shown in Fig. 1.

Figure 2 shows the laser behavior at different time steps for 1 and 5 μm preformed plasma scale length. It shows that the laser is transferring its energy to the particles and reflects backward at the critical density, meaning it can accelerate higher energetic electrons. However, for the case of 5 μm, the laser starts filamenting inside the plasma

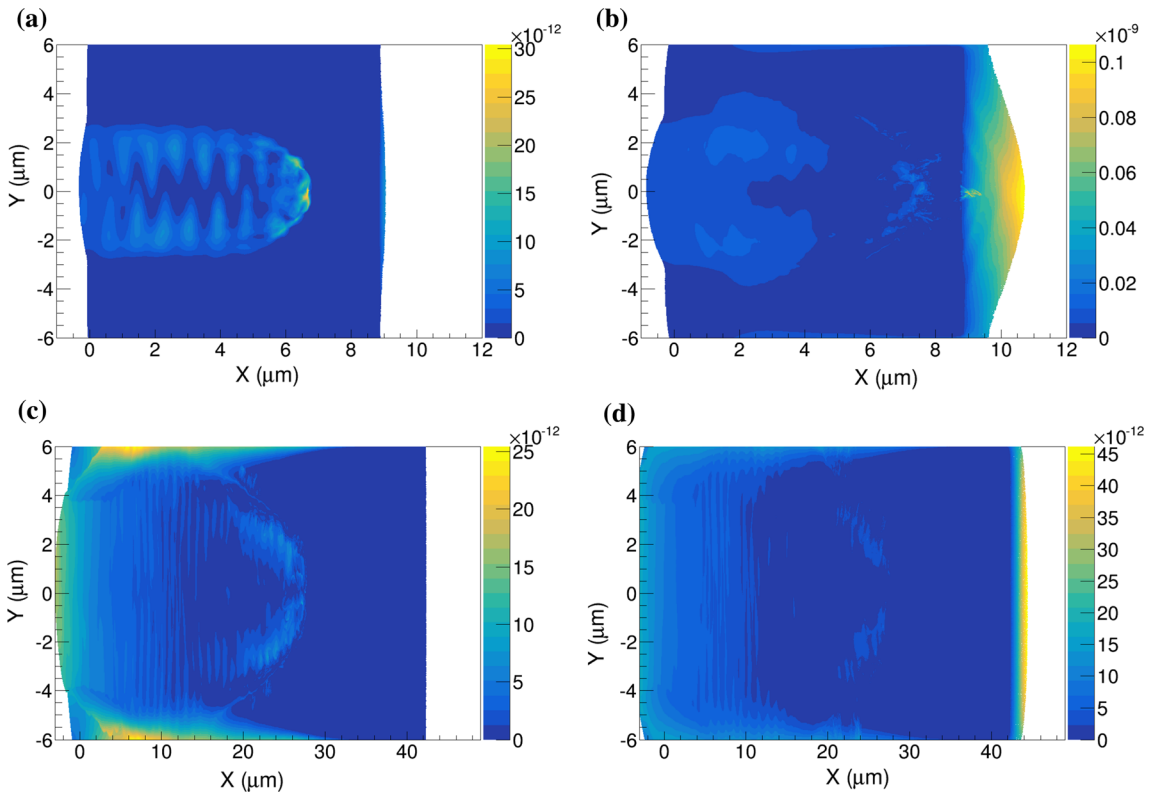

Fig. 1 Average kinetic energy of carbon ions for (**a**) 1 μm scale length at 75 fs and (**b**) 1 μm scale length at 100 fs, (**c**) 5 μm plasma scale length at 200 fs and (**d**) 5 μm scale length at 250 fs time steps, respectively

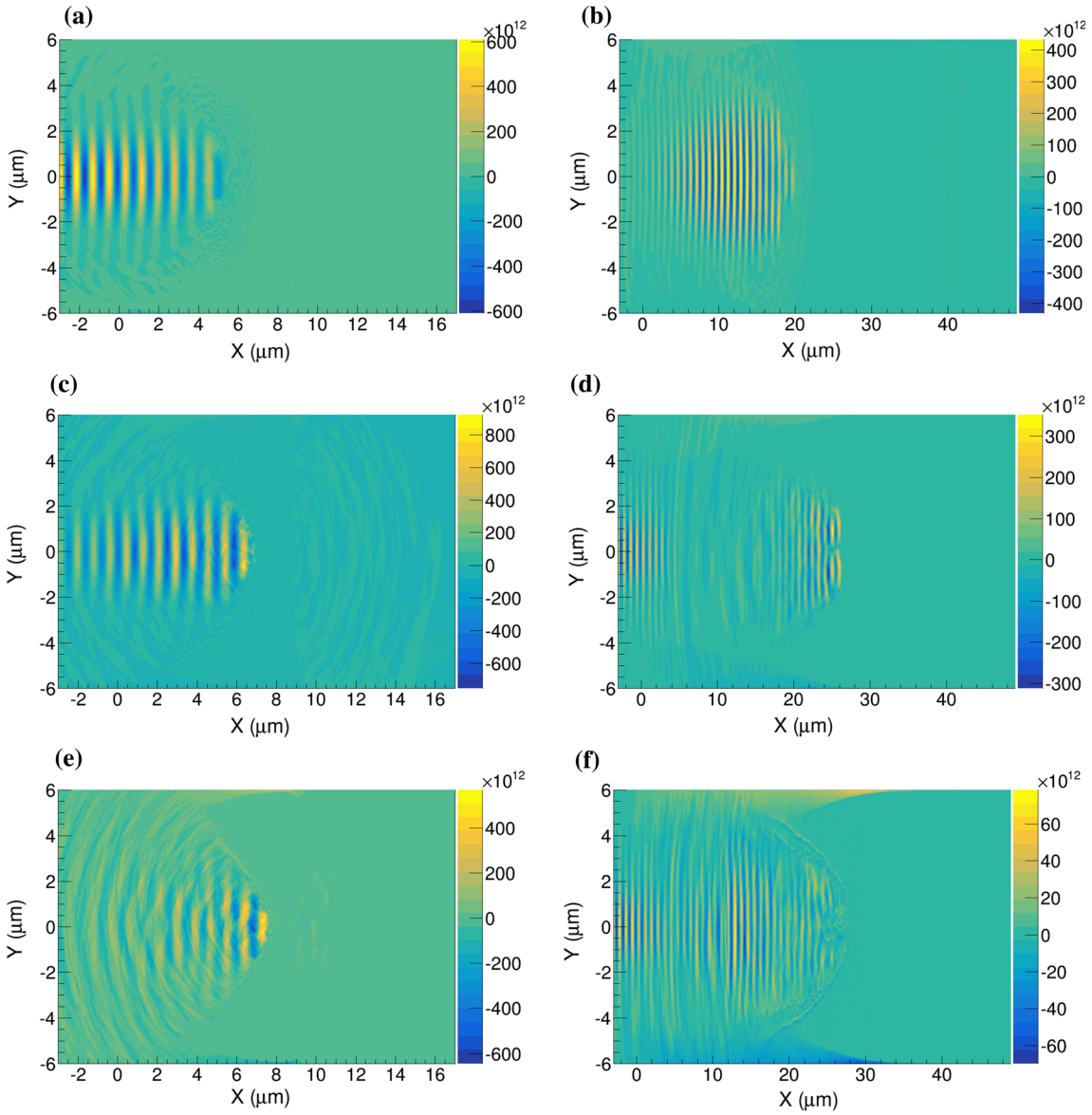

Fig. 2 Laser electric field on the y-direction extracted from 2D PIC simulations for (**a**) 1 μm scale length at 50 fs, (**b**) 5 μm scale length at 100 fs, (**c**) 1 μm scale length at 75 fs, (**d**) 5 μm scale length at 150 fs, (**e**) 1 μm scale length at 100 fs and (**f**) 5 μm scale length at 200 fs when the laser starts reflecting from the critical density

causing a loss of initial laser irradiance. Thus, the laser employed for particle acceleration behaves like a laser with less power and therefore is not efficient at accelerating the particles if it is not totally absorbed inside the plasma as in the 10 μm case. The temperature of generated particles follows the same trend as their maximum energy at the same plasma scale lengths with QED effects.

3. Results and discussion

To understand the effect of plasma density scale length on particle acceleration, electrons, carbon ions and gamma-ray energy spectra were examined. At these irradiances, observation of positron generation with QED effect is not possible. The energy spectra of electrons, ions and gamma rays with preformed plasma at the front surface are shown in Fig. 3 for the plasma scale length of $L = 0, 3, 5$ and 10 μm, respectively. It is seen that adding preformed plasma in front of the target affects the energy of accelerated particles.

From our simulations, we found that there is an optimum scale length for the simulation setup. By controlling the preformed plasma, we can control the energy and temperature of accelerated particles and photons. The results with the absence of QED effect with relatively

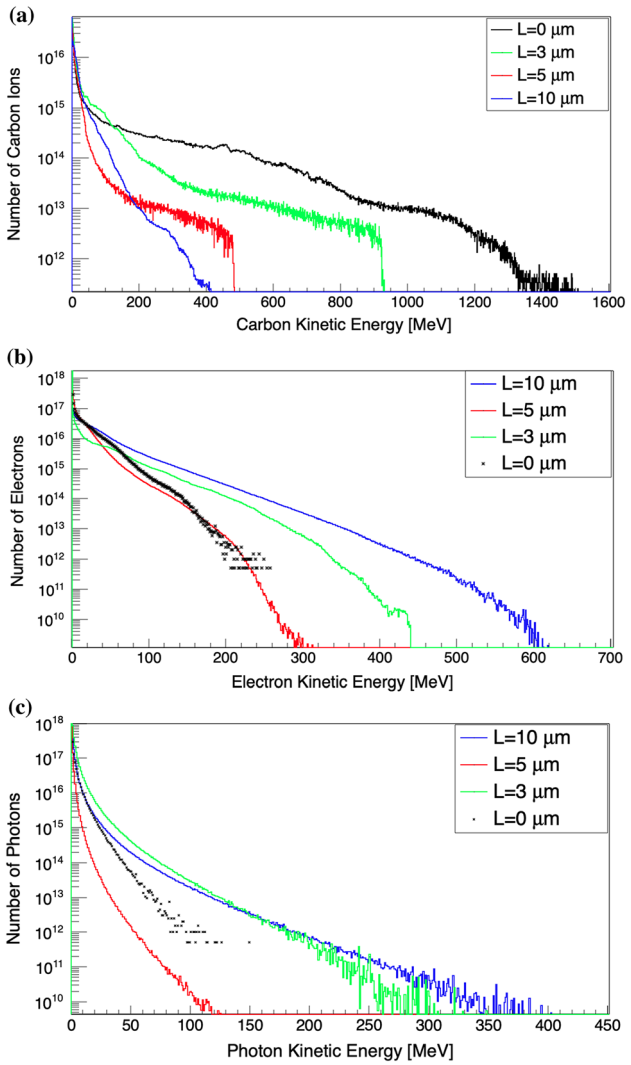

Fig. 3 Kinetic energy spectra of accelerated carbon ions (**a**), electrons (**b**) and photons (**c**) at various plasma scale lengths including QED effects

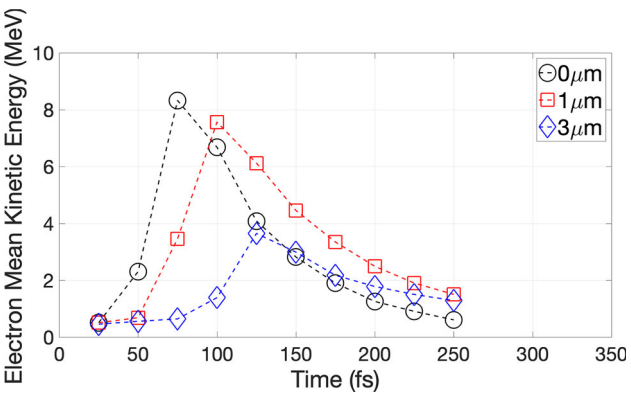

Fig. 4 Average energy of generated electrons as a function of time. Black circle (◯), red squares (□) and blue diamond (◇) represent the average energy at 0, 1 and 3 μm preformed plasma scale lengths, respectively

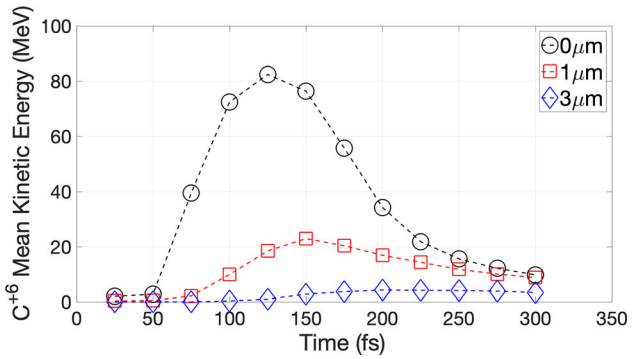

Fig. 5 Average energy of generated C^{+6} ions as a function of time. Black circle (◯), red square (□) and blue diamond (◇) represent the average carbon ion energies at 0, 1 and 3 μm preformed plasma scale lengths, respectively

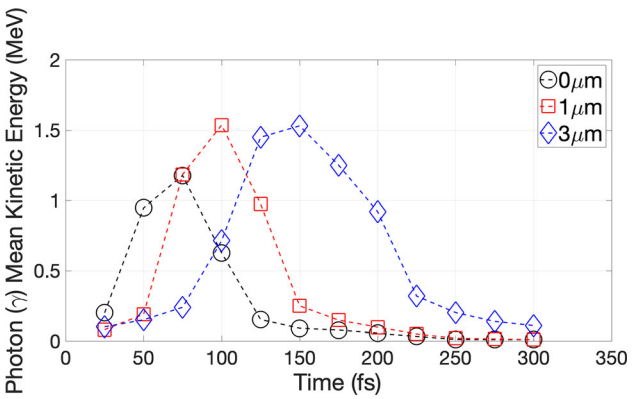

Fig. 6 Average energy of generated gamma beams as a function of time. Black circle (◯), red square (□) and blue diamond (◇) represent the average photon energy at 0, 1 and 3 μm preformed plasma scale lengths, respectively

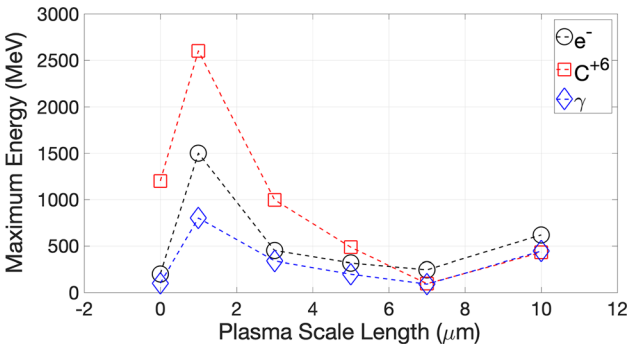

Fig. 7 Maximum energy of generated particles as a function of preformed plasma scale length. Black circle (◯) , red square (□) and blue diamond (◇) represent the electron, carbon ion and photon energies, respectively

lower laser irradiances show more efficient laser absorption, and thus, more energetic particles are produced [23–26] as scale length increases. In this research, it is seen that smaller scale lengths (~ 1 μm) generate more energetic particles. However, increasing scale length reduces

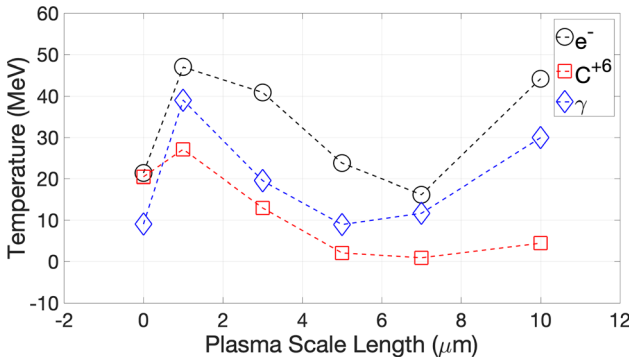

Fig. 8 Extracted temperature of generated particles as a function of preformed plasma scale length. Black circle (◯) represents the hot electron temperature, red square (□) represents the carbon ion temperature per nucleon, and blue diamond (◇) represents the photon temperature

the energy of particles. Additionally, if the plasma scale length is more than 7 μm, particles start gaining energy again with increasing scale length. These results are related to the laser absorption processes in the preformed plasma.

Figure 4 shows the average energy of accelerated electrons inside the plasma for different preformed plasma scale lengths as a function of laser interaction time. We see that adding a preformed plasma results in a higher number of accelerated electrons with less average energy. The laser interaction time at which the maximum average energy is reached changes due to the laser's path to reach the critical density.

Figure 5 shows the average energy of accelerated C^{+6} ions for different preformed plasma scale lengths as a function of laser interaction time. For all plasma scale lengths, the laser first transfers its energy to electrons (the time to reach the maximum average energy is shorter for electrons than carbon ions); then, it accelerates the carbon ions with sheath electric field setup by the TNSA mechanism.

Figure 6 shows the average energy of generated photons as a function of time for different preformed plasma scale lengths. It is seen that preformed plasma in front of the target has a significant impact on number and energy of generated gamma beams. Mainly, increasing scale length reduces the maximum energy up to 7 μm scale length. However, the number and the average energy of generated gamma beams increase with increasing scale length.

The maximum energy and temperature of generated particles with QED effects are summarized as a function of plasma scale length in Figs. 7 and 8, respectively. Since particle energy spectra change for different plasma scale lengths with the presence of QED effects, we determine the particle temperature (kT) by fitting the particle energy spectra with an exponential of the form $\exp(-E/kT)$. The generated particle energy and temperature depend on plasma scale length, as shown in Figs. 7 and 8. For the $L = 1$ μm plasma scale length, we see a clear increase in both measured energy and temperature. This trend on accelerated particle energy is reversed with increasing plasma scale length until $L = 7$ μm, after which the particle energy and temperature start to increase again for all three particle types. The general trend is for plasma scale length effects with the presence of QED effects to decrease the temperature of particles when the preformed plasma is present.

One of the possible explanations for this behavior is that the laser is efficiently absorbed and transfers its energy to electrons. This leads to the acceleration of fast electrons when the plasma scale length is about 1 μm. As the plasma scale length is increased, the laser self-focusing and filamentations inside the plasma reduce the laser intensity. However, if we continue increasing the plasma scale length, all the laser's energy gets absorbed inside the plasma with insignificant amount of back reflection and the laser transfers all its energy to the particles which generate higher energy particles, when compared to lower plasma scale length cases.

For the next-generation laser–solid interactions, adding a preformed plasma in front of the target leads to the generation of more energetic particles compared to the interactions without preformed plasma [27]. With a slight increase in plasma scale length, the energy of generated particles increases, which results in particles with higher temperatures. However, adding more plasma in front of the target can reduce the energy and temperature of the generated particles due to laser filamentations which diminish the laser energy up to some certain scale length where all the laser is absorbed inside the plasma without any back reflection. Thus, higher energy carbon ions up to 2.5 GeV can be produced easily for the new-generation 10 PW laser–plasma interactions.

4. Conclusions

In conclusion, we investigated the effect of plasma scale length with the presence of QED processes on particle acceleration in the next-generation laser–matter interactions with the laser intensity of 5×10^{22} W cm^{-2}. On simulating the case with a preformed plasma at various plasma scale lengths, we found that increasing laser irradiances and adding QED effects to our simulations have similar physical mechanisms to lower laser irradiances. Particle acceleration depends on laser absorption inside the plasma. We showed that increasing plasma scale length can reduce the energy and temperature of accelerated particles up to a certain length due to laser back reflection, self-focusing and filamentation. However, adding a small

amount of preformed plasma in front of the target produces higher energy particles which are important for many applications. We pointed out that the particle energy was reduced due to laser filamentations inside the plasma but in the case of lower scale lengths ($\sim 1\,\mu m$), and the laser transfers its energy to particles without filamenting and reflects backward at the critical density. Finally, we also showed that the created gamma-ray photons with the QED effect also depend on the preformed plasma scale length.

Acknowledgements The research was supported by TUBITAK research Project 116F042 and by Karamanoglu Mehmetbey University Research Project 40-M-16. This work was in part funded by the UK EPSRC Grants EP/G054950/1, EP/G056803/1, EP/G055165/1 EP/M018156/1 and EP/ M022463/1.

References

[1] (2019). http://eli-laser.eu. Accessed 1 Feb 2019
[2] H Daido, M Nishiuchi and A S Pirozhkov *Rep.Prog.Phys.* **75** 056401 (2012)
[3] A Macchi, M Borghesi and M Passoni *Rev. Mod. Phys.* **85** 751 (2013)
[4] S V Bulanov, J J Wilkens, T Zh Esirkepov, *et al. Phys. Uspekhi* **57** 1149 (2014)
[5] C I Blaga, J Xu, A D DiChiara, E Sistrunk, *et al. Nature* **483**, 194 (2011)
[6] T Tajima and J M Dawson *Phys. Rev. Lett.* **43** 267 (1979)
[7] E Esarey, C B Schroeder and W P Leemans *Rev. Mod. Phys.* **81** 1229 (2009)
[8] S Steinke, J Van Tilborg, C Benedetti, *et al Nature* **530** 190 (2016)
[9] B Qiao, S Kar, M Geissler, *et al. Phys. Rev. Lett.* **108** 115002 (2012)
[10] G Breit and J A Wheeler *Phys. Rev.* **46** 1087 (1934)
[11] A R Bell and J G Kirk *Phys. Rev. Lett.* **101** 200403 (2008)
[12] A M Fedotov, N B Narozhny and G Mourou *Phys. Rev. - Lett.* **105** 080402 (2010)
[13] E N Nerush, I Yu Kostyukov, A M Fedotov, *et al. - Phys. Rev. Lett.* **106** 035001 (2011)
[14] I V Sokolov, N M Naumova and J A Nees *Phys. Plasmas* **18** 093109 (2011)
[15] C P Ridgers, C S Brady, R Ducluos, *et al. Phys. Rev. Lett.* **108** 165006 (2012)
[16] M Tamburini, F Pegoraro, A Di Piazza, *et al. New J. Phys.* **12** 123005 (2010)
[17] P Zhang, C P Ridgers and A G R Thomas *New J. Phys.* **17** 043051 (2015)
[18] C P Ridgers, J G Kirk, R Duclous, *et al. J. Comput. Physics* **260** 273 (2014)
[19] T D Arber, K Bennett, C S Brady, *et al. Plasma Phys. Control. Fusion* **57** 113001 (2015)
[20] T Esirkepov, M Borghesi, S V Bulanov, *et al. - Phys. Rev. Lett.* **92** 175003 (2004)
[21] A P L Robinson, M Zepf, S Kar, *et al. New J. Phys.* **10** 013021 (2008)
[22] A Higginson, R J Gray, M King, *et al. Nat. Commun.* **9** 724 (2018)
[23] M I K Santala, M Zeph, I Watts, *et al. Phys. Rev. Lett* **84** 1459 (2000)
[24] J Peebles, M S Wei, A V Arefiev, *et al. New J. Phys.* **19** 023008 (2017)
[25] O Culfa, G J Tallents, A K Rossall, *et al. Phys. Rev. E* **93** 043201 (2016)
[26] O Culfa, G J Tallents, M E Korkmaz, *et al. Laser and Particle Beams* **35** 58 (2017)
[27] T Nakamura, J K Koga, T Zh Esirkepov, *et al. - Phys. Rev. Lett.* **108** 195001 (2012)